PHYSICAL REVIEW E **95**, 051101(R) (2017)

Mechanism of unconfined dust explosions: Turbulent clustering and radiation-induced ignition

Michael Liberman,[1,*] Nathan Kleeorin,[1,2,†] Igor Rogachevskii,[1,2,‡] and Nils Erland L. Haugen[3,4,§]

[1]*Nordita, KTH Royal Institute of Technology and Stockholm University, Roslagstullsbacken 23, 10691 Stockholm, Sweden*

[2]*Department of Mechanical Engineering, Ben-Gurion University of the Negev, P.O. Box 653, Beer-Sheva 84105, Israel*

[3]*SINTEF Energy Research, 7034 Trondheim, Norway*

[4]*Department of Energy and Process Engineering, Norwegian University of Science and Technology, Kolbjørn Hejes vei 1B, 7491 Trondheim, Norway*

(Received 22 September 2016; revised manuscript received 19 April 2017; published 12 May 2017)

It is known that unconfined dust explosions typically start off with a relatively weak primary flame followed by a severe secondary explosion. We show that clustering of dust particles in a temperature stratified turbulent flow ahead of the primary flame may give rise to a significant increase in the radiation penetration length. These particle clusters, even far ahead of the flame, are sufficiently exposed and heated by the radiation from the flame to become ignition kernels capable to ignite a large volume of fuel-air mixtures. This efficiently increases the total flame surface area and the effective combustion speed, defined as the rate of reactant consumption of a given volume. We show that this mechanism explains the high rate of combustion and overpressures required to account for the observed level of damage in unconfined dust explosions, e.g., at the 2005 Buncefield vapor-cloud explosion. The effect of the strong increase of radiation transparency due to turbulent clustering of particles goes beyond the state of the art of the application to dust explosions and has many implications in atmospheric physics and astrophysics.

DOI: 10.1103/PhysRevE.95.051101

I. INTRODUCTION

As is known, dust explosions can occur when an accidentally ignited flame propagates through a cloud of fine particles suspended in a combustible gas. The danger of dust explosions have been known for centuries in the mining industry and grain elevators and it is currently a permanent threat in all those industries in which powders of fine particles are involved. Significant progress has been made in the development of prevention and safety measures (see, e.g., [1–5] and references therein). However, despite considerable effort over more than 100 years, the mechanism of flame propagation in unconfined (large-scale) dust explosions still remains a major unresolved issue.

Based on the analysis of many catastrophic accidents, it is currently well established that unconfined dust explosions consist of a relatively weak primary explosion followed by a severe secondary explosion. While the hazardous effect of the primary explosion is relatively small, the secondary explosion may propagate with a speed of up to 1000 m/s, producing overpressures of over 8–10 atm, which is comparable to the pressures produced by a detonation. However, the analysis of damages indicates that a detonation is not involved, while normal deflagrations are not capable of producing such high velocities and overpressures. It is interesting to note that Faraday and Lyell, who in 1845 analyzed the Haswell coal mine explosion, where the first to point to the likely key role of dust particles [6].

Of special interest for understanding the nature of dust explosions is the Buncefield vapor-cloud explosion, for which a large amount of data and evidence were collected, providing unique and valuable information about the timing and damage caused by the event [7]. Later, a comprehensive analysis was performed by two groups [8,9] in an attempt to understand possible mechanisms leading to the unusually high rate of combustion. Among different mechanisms, the hypothesis proposed by Moore and Weinberg [10,11], where they argue that the anomalously high rate of flame propagation in dust explosions can be due to the radiative ignition of millimeter-sized fibrous particles ahead of the flame front, has attracted much attention.

In normal practice, emissivity of combustion products and radiation absorption in a fresh unburned gaseous mixture are small and do not influence the flame propagation. The situation is drastically changed for flames propagating through a cloud of fine particles suspended in a gaseous mixture. In this case, the radiative flux emitted from the primary flame ($\approx$300–400 kW/m^2) is close to the blackbody radiation [12] at stoichiometric flame temperatures (2200–2500 K). In dust explosions, the radiative flux into the reactants is significantly enhanced by the increased emissivity of the large volume of burned products. Micron-sized dust particles, with diameter d_p that is larger than the radiation wavelength $\lambda_{\rm rad}$, efficiently absorb radiation emitted by the flame. The absorbed heat is transferred to the surrounding gas by thermal conduction, so the gas temperature lags behind that of the particle.

If particles are evenly distributed, the maximum temperature increase ahead of the flame is [13]

$$\Delta T_p \approx \frac{0.63\sigma T_b^4}{U_{\rm f}(\rho_p c_{\rm p} + \rho_g c_{\rm v})}, \tag{1}$$

where $U_{\rm f}$ is the normal flame velocity, σT_b^4 is the blackbody radiative flux, and ρ_p, ρ_g, $c_{\rm p}$, and $c_{\rm v}$ are the mass density of particles, the gas mixture, and their specific heats, respectively. As a flame propagates through a dust cloud of evenly dispersed

*mliber@nordita.org
†nat@bgu.ac.il
‡gary@bgu.ac.il
§nils.e.haugen@sintef.no

particles it consumes the unburned fuel before the gas temperature will have risen to the ignition level, so radiation cannot become a dominant process of the heat transfer [13].

Instead of being uniformly distributed, the particles may be organized in the form of a distant optically thick layer or a clump ahead of the flame front. It was shown [14] that if a transparent gap between the particle layer and the flame is not too small, the particle layer can be sufficiently heated by the flame-emanated radiation to ignite new combustion modes in the surrounding fuel-air mixture ahead of the main flame.

In turbulent flows ahead of the primary flame (Re $\approx 10^4 - 10^5$), typical for dust explosions, dust particles with $\rho_p \gg \rho_g$ assemble in small clusters of the order of the Kolmogorov turbulent scale $\ell_\eta \approx 0.1$–1 mm. The turbulent eddies, acting as small centrifuges, push the particles to the regions between the eddies where the pressure fluctuations are maximum and the vorticity intensity is minimum. The particles assembled in these regions make clusters with higher particle number densities than the mean number density. This effect, known as inertial clustering, has been investigated in a number of analytical, numerical, and experimental studies [15–25].

Recent analytical studies [26,27] and laboratory experiments [28] have shown that the particle clustering can be much more effective in the presence of a mean temperature gradient. In this case, the turbulence is temperature stratified and the turbulent heat flux is not zero. This causes correlations between fluctuations of fluid temperature and velocity and therefore correlations between fluctuations of pressure and fluid velocity, thus producing additional pressure fluctuations caused by the tangling of the mean temperature gradient by the velocity fluctuations. This enhances the particle clustering in the regions of maximum pressure fluctuations. As a result, the particle concentration in clusters rises by a few orders of magnitude compared to the mean concentration of evenly dispersed particles [26].

In order for a secondary dust explosion followed by a shock wave to occur, the pressure from the mixture ahead of the flame ignited by the radiatively heated particle clusters must rise faster than it can be equalized by sound waves. This means that the penetration length of radiation $L_{\rm rad}$ in the dust cloud must be sufficiently large to ensure that the clusters of particles even far ahead of the flame are sufficiently exposed and heated by the radiation to become ignition kernels, i.e., $\tau_{\rm ign} c_{\rm s} \ll L_{\rm rad}$. Here $c_{\rm s}$ is the sound speed in the mixture ahead of the flame and $\tau_{\rm ign}$ is the characteristic time of fuel-air ignition by the radiatively heated particle clusters (ignition kernels). The effect of spatial inhomogeneities with scales larger than the wavelength of the radiation has been discussed in [29–31] and studied using Monte Carlo modeling [32,33] of the radiative heat transfer in particle-laden flow, taking into account the inertial particle clustering in nonstratified turbulence.

In this paper we show that clustering of particles ahead of the primary flame gives rise to a strong increase of the radiation penetration (absorption) length. The effect ensures that clusters of particles even far ahead of the primary flame are sufficiently exposed and heated by the radiation from the flame to become ignition kernels and the condition $\tau_{\rm ign} c_{\rm s} \ll L_{\rm rad}$ is satisfied. The multiple radiation-induced ignitions in many ignition kernels ahead of the primary flame increase the total flame surface area, so the distance that each flame has to cover for a complete burnout of the fuel is substantially reduced. This results in a strong increase of the effective combustion speed, defined as the rate of reactant consumption of a given volume. The proposed mechanism of unconfined dust explosions explains the physics behind the secondary explosion. It also explains the anomalously high rate of combustion and overpressures required to account for the observed level of damage in unconfined dust explosions.

II. MEAN-FIELD EQUATION FOR RADIATION TRANSFER

To describe this phenomenon, we consider a turbulent flow with suspended particles that is exposed to a radiative flux. The radiative transfer equation in the two-phase flow [34,35] for the intensity of radiation $I(\boldsymbol{r},\hat{\boldsymbol{s}})$ is

$$(\hat{\boldsymbol{s}}\cdot\boldsymbol{\nabla})I(\boldsymbol{r},\hat{\boldsymbol{s}}) = -[\kappa_g(\boldsymbol{r})+\kappa_p(\boldsymbol{r})+\kappa_s(\boldsymbol{r})]I(\boldsymbol{r},\hat{\boldsymbol{s}}) + \kappa_g I_{b,g} + \kappa_p I_{b,p} + \frac{\kappa_s}{4\pi}\int \phi(\boldsymbol{r},\hat{\boldsymbol{s}},\hat{\boldsymbol{s}}')I(\boldsymbol{r},\hat{\boldsymbol{s}}')d\Omega, \quad (2)$$

where $\kappa_g(\boldsymbol{r})$ and $\kappa_p(\boldsymbol{r})$ are the absorption coefficients of the gas and particles, respectively, $\kappa_s(\boldsymbol{r})$ is the particle scattering coefficient, ϕ is the scattering phase function, $I_{b,g}(\boldsymbol{r})$ and $I_{b,p}(\boldsymbol{r})$ are the blackbody emission intensities for the gas and particles, respectively, which depend on the local temperature, $\hat{\boldsymbol{s}} = \boldsymbol{k}/k$ is the unit vector in the direction of radiation, $\boldsymbol{k}$ is the wave vector, $\boldsymbol{r}$ is the position vector, $d\Omega = \sin\theta\, d\theta\, d\varphi$, and (k,θ,φ) are the spherical coordinates in $\boldsymbol{k}$ space. Since the scattering and absorption cross sections for gases at normal conditions are very small, the contribution from the gas phase can be neglected in comparison with that of particles. Furthermore, we assume that the particle absorption coefficient is much larger than the scattering coefficient $|\kappa_p(\boldsymbol{r})| \gg |\kappa_s(\boldsymbol{r})|$, which is the case when $\pi d_p\sqrt{|\epsilon|}/\lambda_{\rm rad} \gg 1$ [36], where ϵ is the dielectric permeability of the dust particles, $\lambda_{\rm rad}$ is the radiation wavelength, and d_p is the diameter of the dust particles. Under these assumptions Eq. (2) is reduced to

$$(\hat{\boldsymbol{s}}\cdot\boldsymbol{\nabla})I(\boldsymbol{r},\hat{\boldsymbol{s}}) = -\kappa(\boldsymbol{r})[I(\boldsymbol{r}) - I_b], \quad (3)$$

where we define $\kappa \equiv \kappa_p(\boldsymbol{r})$ and $I_b \equiv I_{b,p}$.

The radiation absorption length of evenly dispersed particles is $L_a = 1/\overline{\kappa}$, where $\overline{\kappa} = \sigma_a \overline{N}$ is the mean particle absorption coefficient, $\sigma_a \approx \pi d_p^2/4$ is the particle absorption cross section, and $\overline{N}$ is the mean number density of evenly dispersed particles. For a typical mean dust density $\overline{\rho}_d \equiv \overline{N} m_{\rm p} = 0.1$–$0.3\,{\rm kg/m^3}$, the corresponding radiation absorption length is $L_a = 1/\overline{\kappa} \approx (\rho_p/2\rho_d)d_p \approx 10$ cm, where $\rho_p = 1\ {\rm kg/cm^3}$ and $d_p = 10\,\mu$m. If particles are accumulated in optically thick clusters, with the particle number density within clusters $n_{\rm cl}$ much larger than $\overline{N}$, the effective radiation absorption length can be roughly estimated as $L_{\rm eff} = 1/\sigma_{\rm cl} N_{\rm cl}$, where $\sigma_{\rm cl}$ is the cluster cross section and $N_{\rm cl}$ is the mean number density of clusters. Taking into account that the cluster size is of the order of the Kolmogorov turbulent scale ℓ_η, we obtain $L_{\rm eff}/L_a \approx (n_{\rm cl}/\overline{N})(\ell_\eta/L_a)$. This expression shows that the result depends on the interplay between a large factor $n_{\rm cl}/\overline{N} \gg 1$ and a small factor $\ell_\eta/L_a \ll 1$, which in turn depend on the parameters of turbulence.

To determine the effective radiation absorption coefficient for a turbulent flow with particle clustering, we apply a mean-field approach, i.e., all quantities are decomposed into the mean and fluctuating parts $I = \overline{I} + I'$, $I_b = \overline{I}_b + I'_b$, and $\kappa = \overline{\kappa} + \kappa'$, where the fluctuating parts I', I'_b, and κ' have zero mean values and overbars denote averaging over an ensemble. The instantaneous particle absorption coefficient is $\kappa = n\sigma_a$ and the mean particle absorption coefficient is $\overline{\kappa} = \overline{N}\sigma_a$, so the fluctuations of the particle absorption coefficient are $\kappa' = n'\sigma_a = n'\overline{\kappa}/\overline{N}$. Here $n = \overline{N} + n'$ is the instantaneous particle number density and n' are fluctuations of the particle number density.

We average Eq. (3) over the ensemble of the particle number density fluctuations and assume that the characteristic correlation scales of fluctuations are much smaller than the scales of the mean-field variations. The equation for the mean radiation intensity $\overline{I}(\boldsymbol{r},\hat{\boldsymbol{s}})$ reads

$$(\hat{\boldsymbol{s}}\cdot\nabla)\overline{I}(\boldsymbol{r},\hat{\boldsymbol{s}}) = -\overline{\kappa}(\overline{I} - \overline{I}_b) - \langle\kappa' I'\rangle + \langle\kappa' I'_b\rangle, \qquad (4)$$

where the angular brackets denote averaging over an ensemble of fluctuations. To determine the one-point correlation function $\langle\kappa' I'\rangle$, we need to derive equations for fluctuations I' and κ'. By subtracting Eq. (4) from Eq. (3) we obtain the equation for fluctuations of I',

$$(\hat{\boldsymbol{s}}\cdot\nabla + \overline{\kappa} + \kappa')I'(\boldsymbol{r},\hat{\boldsymbol{s}}) = I_{\rm source}, \qquad (5)$$

where the source term is

$$I_{\rm source} = -\kappa'(\overline{I} - \overline{I}_b) + \langle\kappa' I'\rangle + (\overline{\kappa} + \kappa')I'_b - \langle\kappa' I'_b\rangle. \qquad (6)$$

The solution of Eq. (5) reads

$$I'(\boldsymbol{r},\hat{\boldsymbol{s}}) = \int_{-\infty}^{\infty} I_{\rm source}\exp\left[-\left|\int_{s'}^{s}[\overline{\kappa} + \kappa'(s'')]ds''\right|\right]ds', \qquad (7)$$

where $s = \boldsymbol{r}\cdot\hat{\boldsymbol{s}}$. Expanding the function $\exp[-|\int_{s'}^{s}\kappa'(s'')|ds'']$ in a Taylor series, multiplying Eq. (7) by κ', and averaging over the ensemble of fluctuations, we obtain the following equation for the one-point correlation function $\langle\kappa' I'\rangle$:

$$\langle\kappa' I'\rangle = -\overline{\kappa}(\overline{I} - \overline{I}_b)\frac{2\beta J_1}{1 + 2\beta J_2}, \qquad (8)$$

where $\beta = \overline{\kappa}\ell_D$ and $\ell_D = a\ell_\eta/{\rm Sc}^{1/2}$ with a numerical coefficient $a \gg 1$, while the Schmidt number is given by ${\rm Sc} = \nu/D$, ν is the kinematic viscosity, D is the coefficient of the Brownian diffusion of particles,

$$J_1 = \int_0^{\infty}\Phi(Z)\exp(-\beta Z)dZ, \qquad (9)$$

$$J_2 = \beta\int_0^{\infty}\left(\int_0^{Z}\Phi(Z')dZ'\right)\exp(-\beta Z)dZ, \qquad (10)$$

and $\Phi(\mathbf{R}) = \langle n'(\mathbf{x})n'(\mathbf{x}+\mathbf{R})\rangle$ is the two-point instantaneous correlation function of the particle number density fluctuations. In the derivation of Eq. (8) we applied the quasilinear approach, i.e., we neglected the third and higher moments in fluctuations of κ' in Eq. (8) due to a small parameter $\kappa'\ell_\eta{\rm Sc}^{-1/2} \ll 1$. We also assumed that $\langle\kappa' I'_b\rangle = 0$, i.e., we neglected the correlation between the particle number density fluctuations and the fluid temperature fluctuations.

Substituting Eq. (8) for $\langle\kappa' I'\rangle$ into Eq. (4), we obtain the mean-field equation for the mean radiation intensity

$$(\hat{\boldsymbol{s}}\cdot\nabla)\overline{I}(\boldsymbol{r},\hat{\boldsymbol{s}}) = -\kappa_{\rm eff}(\overline{I} - \overline{I}_b), \qquad (11)$$

where the effective absorption coefficient $\kappa_{\rm eff}$ is

$$\kappa_{\rm eff} = \overline{\kappa}\left(1 - \frac{2\beta J_1}{1 + 2\beta J_2}\right). \qquad (12)$$

The last term on the right-hand side of Eq. (12) takes into account the particle clustering in stratified turbulence.

III. PARTICLE CORRELATION FUNCTION

To calculate the integrals J_1 and J_2, we use the normalized two-point correlation function of the particle number density fluctuations $\Phi(R) = \langle n'(\boldsymbol{r})n'(\boldsymbol{r}+\boldsymbol{R})\rangle/\overline{N}^2$, derived in [26] for a temperature stratified turbulence $\Phi(R) = (n_{\rm cl}/\overline{N})^2$ for $0 \leqslant R \leqslant \ell_D$ and

$$\Phi(R) = \left(\frac{n_{\rm cl}}{\overline{N}}\right)^2\left(\frac{R}{\ell_D}\right)^{-\mu}\cos\left[\alpha\ln\left(\frac{R}{\ell_D}\right)\right] \qquad (13)$$

for $\ell_D \leqslant R \leqslant \infty$, where $R = \boldsymbol{R}\cdot\hat{\boldsymbol{s}}$ and

$$\mu = \frac{1}{2(1+3\sigma_T)}\left[3 - \sigma_T + \frac{20\sigma_v(1+\sigma_T)}{1+\sigma_v}\right], \qquad (14)$$

$$\alpha = \frac{3\pi(1+\sigma_T)}{(1+3\sigma_T)\ln{\rm Sc}}. \qquad (15)$$

Here $\sigma_T = (\sigma_{T0}^2 + \sigma_v^2)^{1/2}$ is the degree of compressibility of the turbulent diffusion tensor and σ_v is the degree of compressibility of the particle velocity field:

$$\sigma_v = \frac{8\,{\rm St}^2K^2}{3(1 + b\,{\rm St}^2K^2)}, \quad K = \left[1 + {\rm Re}\left(\frac{L_*\nabla\overline{T}}{\overline{T}}\right)^2\right]^{1/2}, \qquad (16)$$

where ${\rm Re} = \ell_0 u_0/\nu$ is the Reynolds number, $\sigma_{T0} = \sigma_T({\rm St}=0)$, and a constant b determines the value of the parameter σ_v in the limit of ${\rm St}^2K^2 \gg 1$. The ratio of the particle Stokes time $\tau_p = m_p/3\pi\rho\nu d_p$ and the Kolmogorov time $\tau_\eta = \tau_0/{\rm Re}^{1/2}$ is the Stokes number ${\rm St} = \tau_p/\tau_\eta$, where $\tau_0 = \ell_0/u_0$ and u_0 are the characteristic time and velocity at the turbulent integral scale ℓ_0, respectively. In Eq. (16), $\overline{T}$ is the mean fluid temperature and the length $L_* = c_s^2\tau_\eta^{3/2}/9\nu^{1/2}$.

To derive Eqs. (13)–(16) we used Eqs. (42)–(47) in [26] and Eqs. (17) and (18) in [27]. The correlation function $\Phi(R)$ takes into account particle clustering. For the inertial clustering in a nonstratified turbulence $K = 1$, while for the temperature stratified turbulence the nondimensional function K is determined by Eq. (16).

IV. EFFECTIVE RADIATION LENGTH

Integrals J_1 and J_2 are calculated using Eqs. (13)–(16) and taking into account that $\beta = \overline{\kappa}\ell_D \ll 1$,

$$J_1 = J_2 = \left(\frac{n_{\rm cl}}{\overline{N}}\right)^2\left[1 + \frac{\mu - 1}{(\mu-1)^2 + \alpha^2}\right]. \qquad (17)$$

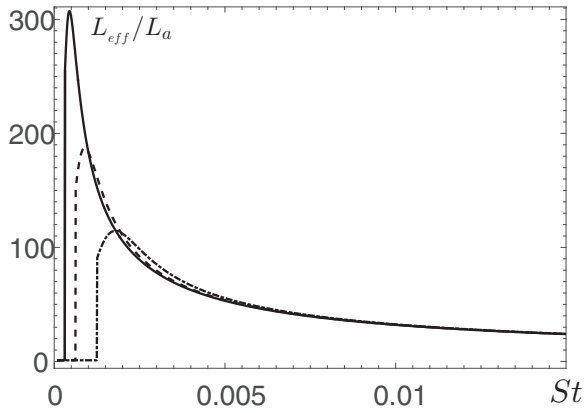

FIG. 1. Ratio $L_{\rm eff}/L_a$ versus the Stokes number St for different mean temperature gradients $|\nabla\overline{T}|$: 0.225 K/m (dash-dotted line), 0.45 K/m (dashed line), and 0.9 K/m (solid line).

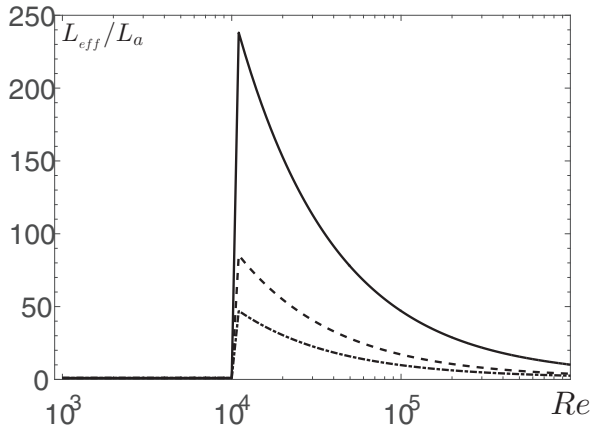

FIG. 2. Ratio $L_{\rm eff}/L_a$ versus the Reynolds number Re for the temperature gradients $|\nabla\overline{T}| = 0.9$ K/m and different particle diameter d_p: 3 μm (solid line), 6 μm (dashed line), and 9 μm (dash-dotted line).

Substituting Eq. (17) into Eq. (12), we determine the effective penetration length of radiation $L_{\rm eff} \equiv 1/\kappa_{\rm eff}$ as

$$\frac{L_{\rm eff}}{L_a} = 1 + \frac{2a}{{\rm Sc}^{1/2}}\left(\frac{n_{\rm cl}}{\overline{N}}\right)^2\left(\frac{\ell_\eta}{L_a}\right)\left[1 + \frac{\mu - 1}{(\mu-1)^2 + \alpha^2}\right]. \quad (18)$$

Figure 1 shows the ratio $L_{\rm eff}/L_a$ versus the Stokes number St for different temperature gradients $|\nabla\overline{T}|$, calculated for parameters typical for unconfined dust explosions: ${\rm Re} = 5 \times 10^4$, $\ell_0 = 1$ m, $u_0 = 1$ m/s, $\nu = 0.2$ cm/s^2, $c_{\rm s} = 450$ m/s for the methane-air mixture, $n_{\rm cl}/\overline{N} = 500$, and $\sigma_{T0} = 1/2$. Using asymptotic analysis we choose $a = 10$ and $b = 5$. Figure 2 shows the ratio $L_{\rm eff}/L_a$ versus the Reynolds numbers for particles of different diameters.

V. DISCUSSION

It is shown that clustering of particles in the temperature stratified turbulent flow ahead of the primary flame gives rise to a strong increase of the radiation penetration length (Fig. 1), but within a narrow interval of turbulent parameters (see Fig. 2). This explains the mechanism of the secondary explosion in unconfined dust explosions. According to analysis of the Buncefield explosion [8], "The high overpressures in the cloud and low average rate of flame advance can be reconciled if the rate of flame advance was episodic, with periods of very rapid combustion being punctuated by pauses when the flame advanced very slowly." Assuming $L_a \sim 10$ cm, we obtain $L_{\rm eff} \sim 10$ m as the result of the turbulent clustering of dust particles. Given that the radiative flux from the primary flame is about $S \sim 300$–$400\,{\rm kW/m^2}$, the temperature of particles increases up to the ignition level $\Delta T_p \approx 1000$ K during $\tau_{\rm ign} = \rho_p d_p c_{\rm p} \Delta T_p/2S < 10$ ms. Time scales of the fuel-air ignition by the radiatively heated cluster of particles (with d_p in the range from 1 to 20 μm) can be smaller than 10 ms [13,37]. This ensures that the condition $L_{\rm eff} \gg c_{\rm s}\tau_{\rm ign}$ is satisfied, and the pressure produced by the ignition of the fuel-air mixture rises until the pressure wave steepens into a shock wave. The effective rate of the secondary explosion propagation is $\sim$1000 m/s, which corresponds to a Mach number Ma = 2.5–3 and overpressures of 8–10 atm. This explains the level of damage observed in the aftermath of unconfined dust explosions [7,8]. At the same time, the secondary explosion strongly change the parameters of the turbulent flow. As a result, rapid combustion in the secondary explosion is interrupted until the shock wave dissipates and the slow combustion parameters of the turbulent flow ahead of a slow deflagration wave will be suitable for formation of a new transparent radiation window. This agrees fairly well with the Buncefield explosion scenario [8]. The effect of the strong increase of the radiation penetration length due to turbulent particle clustering goes beyond the dust explosion applications and has many implications in astrophysical and atmospheric turbulence [27,38,39].

ACKNOWLEDGMENTS

This work was supported by the Research Council of Norway under the FRINATEK (Grant No. 231444). The support of this work provided by the opening Project Number KFJJ17-08M of State Key Laboratory of Explosion Science and Technology, Beijing Institute of Technology is gratefully acknowledged (ML). Stimulating discussions with participants of the NORDITA program on "Physics of Turbulent Combustion" are acknowledged.

[1] R. K. Eckhoff, *Dust Explosions in Process Industries*, 3rd ed. (Gulf Professional, Houston, 2003).
[2] P. R. Amyotte and R. K. Eckhoff, J. Chem. Health Safety **17**, 15 (2010).
[3] C. Proust, J. Loss Prev. Process Ind. **19**, 104 (2006).
[4] T. Abbasi and S. Abbasi, J. Hazardous Mater. **140**, 7 (2007).
[5] Z. Yuan, N. Khakzada, F. Khana, and P. Amyotte, Proc. Safety Environ. Protect. **98**, 57 (2015).

[6] M. Faraday and C. Lyell, Philos. Mag. **26**, 16 (1845).
[7] Buncefield explosion mechanism phase 1, Health and Safety Executive Research Report No. RR718, 2009 (unpublished), Vol. 1-2, available at http://www.buncefieldinvestigation.gov.uk
[8] G. Atkinson and L. Cusco, Process Safety Environ. **89**, 360 (2011).
[9] D. Bradeley, G. A. Chamberlain, and D. D. Drysdale, Philos. Trans. R. Soc. A **370**, 544 (2012).
[10] S. R. Moore and F. J. Weinberg, Nature (London) **290**, 39 (1981).
[11] S. R. Moore and F. J. Weinberg, Proc. R. Soc. London Ser. A **385**, 373 (1983).
[12] M. A. Hadjipanayis, F. Beyrau, R. P. Lindstedt, G. Atkinson, and L. Cusco, Process Safety Environ. Protect. **94**, 517 (2015).
[13] M. A. Liberman, M. F. Ivanov, and A. D. Kiverin, Acta Astronaut. **115**, 82 (2015).
[14] M. A. Liberman, M. F. Ivanov, and A. D. Kiverin, J. Loss Prev. Process Ind. **38**, 176 (2015).
[15] F. Toschi and E. Bodenschatz, Annu. Rev. Fluid Mech. **41**, 375 (2009).
[16] Z. Warhaft, Fluid Dyn. Res. **41**, 011201 (2009).
[17] S. Balachandar and J. K. Eaton, Annu. Rev. Fluid Mech. **42**, 111 (2010).
[18] T. Elperin, N. Kleeorin, and I. Rogachevskii, Phys. Rev. Lett. **77**, 5373 (1996).
[19] T. Elperin, N. Kleeorin, V. S. L'vov, I. Rogachevskii, and D. Sokoloff, Phys. Rev. E **66**, 036302 (2002).
[20] T. Elperin, N. Kleeorin, M. A. Liberman, V. S. L'vov, and I. Rogachevskii, Environ. Fluid Mech. **7**, 173 (2007).
[21] J. Bec, L. Biferale, M. Cencini, A. Lanotte, S. Musacchio, and F. Toschi, Phys. Rev. Lett. **98**, 084502 (2007).
[22] J. Salazar, J. de Jong, L. Cao, S. Woodward, H. Meng, and L. Collins, J. Fluid Mech. **600**, 245 (2008).
[23] H. Xu and E. Bodenschatz, Physica D **237**, 2095 (2008).
[24] E. W. Saw, R. A. Shaw, S. Ayyalasomayajula, P. Y. Chuang, and A. Gylfason, Phys. Rev. Lett. **100**, 214501 (2008).
[25] E. W. Saw, G. P. Bewley, E. Bodenschatz, R. S. Sankar, and J. Bec, Phys. Fluids **26**, 111702 (2014).
[26] T. Elperin, N. Kleeorin, M. A. Liberman, and I. Rogachevskii, Phys. Fluids **25**, 085104 (2013).
[27] T. Elperin, N. Kleeorin, B. Krasovitov, M. Kulmala, M. A. Liberman, I. Rogachevskii, and S. Zilitinkevich, Phys. Rev. E **92**, 013012 (2015).
[28] A. Eidelman, T. Elperin, N. Kleeorin, B. Melnik, and I. Rogachevskii, Phys. Rev. E **81**, 056313 (2010).
[29] Y. A. Kravtsov, Appl. Opt. **32**, 2681 (1993).
[30] L. A. Apresyan and Y. A. Kravtsov, *Radiation Transfer* (Gordon & Breach, Amsterdam, 1996).
[31] N. I. Kliorin, Y. A. Kravtsov, A. E. Mereminskii, and V. G. Mirovskii, Radiophys. Quantum Electron. **32**, 793 (1989).
[32] E. Farbar, I. D. Boyd, and M. Esmaily-Moghadam, J. Quantum Spectrosc. Radiat. Transfer **184**, 146 (2016).
[33] A. Frankel, G. Iaccarino, and A. Mani, J. Quantum Spectrosc. Radiat. Transfer **182**, 45 (2016).
[34] R. Siegel and J. R. Howell, *Thermal Radiation Heat Transfer* (McGraw-Hill, New York, 1981).
[35] Y. B. Zeldovich and Y. P. Raizer, *Physics of Shock Waves and High-Temperature Phenomena* (Academic, New York, 1966).
[36] R. G. Newton, *Scattering Theory of Waves and Particles* (Springer, New York, 1982).
[37] F. Beyrau, M. A. Hadjipanayis, and R. P. Lindstedt, Proc. Combust. Inst. **34**, 2065 (2013).
[38] S. P. Owocki and N. J. Shaviv, Mon. Not. R. Astron. Soc. **462**, 345 (2016).
[39] J. O. Sundqvist, S. P. Owocki, D. H. Cohen, M. A. Leutenegger, and R. H. D. Townsend, Mon. Not. R. Astron. Soc. **420**, 1553 (2012).